THE ASTROPHYSICAL JOURNAL, 462:376–385, 1996 May 1

A THEORETICAL ANALYSIS OF PULSATION DRIVING IN PG 1159 STARS

P. A. BRADLEY
XTA, MS B220, Los Alamos National Laboratory, Los Alamos, NM 87545
AND
W. A. DZIEMBOWSKI
Copernicus Astronomical Center, Polish Academy of Sciences, ul. Bartycka 18, 00-716 Warsaw, Poland
Received 1995 August 18; accepted 1995 November 3

ABSTRACT

Our understanding of stars of the PG 1159 spectral type is not yet satisfactory, in spite of the recent success of asteroseismology. Kawaler and coworkers match the observed pulsation frequencies of PG 1159−035 and PG 2131+066 quite well with evolutionary models, but they fail to identify the mechanism exciting their pulsations. Stanghellini, Cox, & Starrfield show that the classical κ, γ mechanism acting in the C/O partial ionization zone can excite certain g-modes but requires compositions that seem unrealistic. Here we study the impact of the new OPAL opacities on the conditions required to drive the modes observed in the PG 1159 spectral class stars. To this end, we present the nonadiabatic pulsation results of a parametric survey of quasi-evolutionary models of PG 1159 pre–white dwarfs. We examine the effect of varying the chemical composition of the driving region, the stellar radius, and stellar mass on the location of the instability strip and the maximum unstable period. Changes in the oxygen mass fraction of the driving region and the stellar radius have a strong effect on the predicted spectrum of unstable modes.

We do not find unstable modes with periods longer than 150 s unless the driving region, located near $10^{-9}\ M_*$, has at least 50% oxygen. The maximum unstable period increases by factors of 2–3 when we increase the radius of our models by 40%–50%. Decreasing the stellar mass also increases the radius, and the maximum unstable period increases from ~300–400 s at 0.65 $M_\odot$ to ~800 s at 0.50 $M_\odot$ for models with 50:50 C/O cores. Based on these results, we suggest that no pulsating PG 1159 star has a driving region with photospheric abundances; rather they are probably oxygen-rich. In addition, we believe PG 1159−035 and PG 1707+427 probably have larger radii than the seismological models of Kawaler & Bradley predict, because our evolutionary models with pure oxygen cores fail to predict unstable modes with periods up to the ~1000 s we observe. Models with larger radii also have rates of period change closer to that observed for the 516 s mode of PG 1159−035. In contrast, our present 50:50 C/O evolutionary models are able to duplicate the observed maximum unstable periods of the two coolest pulsating PG 1159 stars, PG 2131+066 and PG 0122+200. This suggests that the last two stars have radii close to that predicted by our models, and that their driving regions are less oxygen-rich than in the hotter pulsating PG 1159 stars.

Subject headings: stars: evolution — stars: oscillations — white dwarfs

1. INTRODUCTION

The PG 1159 stars are pre–white dwarfs that lie just below planetary nebula nuclei (PNNs) on the H-R diagram. Located at about log $(L/L_\odot) = 2$, these stars are not yet fully degenerate in their interiors, like white dwarfs. Although they are descendants of PNNs, only recently have we detected traces of a surrounding nebula, in spite of deep imaging surveys done by Reynolds (1987), Méndez et al. (1988), and Kwitter et al. (1989). The recent discovery of large, faint nebulae around RXJ 2117+2412 by Appleton, Kawaler, & Eitter (1993) and around PG 1520+525 by Jacoby & Van De Steene (1995) offers strong support to the idea that PG 1159 stars descend from PNNs, especially since both are among the hottest and most luminous PG 1159 stars. The PG 1159 stars are distinguished spectroscopically by lines of ionized He, C, and O; trace amounts of nitrogen and neon are occasionally seen. The photospheric abundances of PG 1159−035 are typical of the class; its abundances are 33:50:17 He/C/O by mass (Werner 1993). None of these stars show detectable hydrogen lines, but the high effective temperatures (~100,000 K) leave hydrogen so highly ionized that only the upper limit of $n(\mathrm{He})/n(\mathrm{H}) \sim 5$ is possible (Werner 1995).

About half the members of the PG 1159 spectroscopic class, including the PNNs with PG 1159 star spectra, pulsate. The pulsating PG 1159 stars are known as GW Vir (or DOV) stars, while the pulsating planetary nebula nuclei are called PNNV (or KS Dra) stars.[1] These stars are multiperiodic g-mode pulsators, with dominant quasi-periods ranging from around 1500 s for the PNNV stars to about 400 s for the coolest GW Vir stars. These stars offer vital clues to the interior structure of hydrogen-deficient PNNs and their immediate descendants, where the star's structure changes dramatically as it rapidly evolves to become a white dwarf, as Kawaler & Bradley (1994, hereafter KB) describe. In spite of considerable success in modeling the structure of these stars via asteroseismology (Winget et al. 1991; KB; Kawaler et al. 1995), the structure of the driving region is poorly known. The observed periods are insensitive to the structure of the driving region because the eigenfunctions have very little weight there.

Spectroscopic observations only deepen the mystery concerning the driving mechanism responsible for the observed

[1] K. Werner (1995, private communication) suggests using DOV and [WC]V instead to distinguish between the spectral types, rather than going by location in the H-R diagram.

pulsations, because there are no clear photospheric abundance differences between the pulsators and nonpulsators. For example, the nonpulsator PG 1520+525 has identical abundances and a slightly hotter effective temperature (150,000 K; Werner et al. 1995) than PG 1159−035 (at 140,000 K), which is the prototype GW Vir star. Another unsettling mystery is the identical abundances of PG 1159−035 and PG 1707+427, in spite of about 10^5 yr of evolutionary cooling separating the two stars. This evolutionary timescale is much longer than diffusion timescales (a few years at most) in the outer layers, suggesting that something keeps the heavier elements from settling. Radiative levitation cannot be solely responsible, as the observed C and O abundances are too large (Vauclair 1989, 1990). The most likely possibility is the presence of a surface convection zone, along with weak mass loss. Clearly, something is different in the driving regions of these stars that does not show up at the photosphere.

Constraining the driving region chemical composition in the pulsating PG 1159 stars is important for constraining the structure of their outermost layers. Studying the nonadiabatic pulsation properties of models and comparing them to the observed period spectrum may be our best way to constrain the composition of the driving region, because the pulsation period distribution is not significantly affected by the driving region composition. Theory suggests the most likely driving mechanism is a partial ionization zone composed of a mixture of carbon and oxygen. Stanghellini, Cox, & Starrfield (1991) provide the latest analysis of the nonadiabatic pulsation properties of various post–asymptotic giant branch (post–AGB) structure models. Their analysis shows that if helium comprises more than 10%–20% of the material in the driving region, the models are pulsationally stable in the effective-temperature region occupied by the PG 1159 stars. They also find the instability strip for pure oxygen driving regions is hotter than for pure carbon driving regions. Additional details based on earlier models may be found in Starrfield et al. (1983, 1984, 1985) and Cox (1986). Because theoretical periods of pulsation modes are not strongly affected by the composition of the driving region, the strongest observational constraints on the driving region composition are the location of the instability strip and the period spectrum of unstable modes present for a given spherical harmonic index (l) value. Observations show that the longest period unstable mode ($P_{\max}$) is evolution-dependent, ranging from $\gtrsim$2000 s for the PNNV stars to about 500 s for PG 2131+066. The period region of the largest amplitude modes also decreases with decreasing effective temperature; RXJ 2117+34 has its largest amplitude modes around 1000 s, dropping to about 520 s for PG 1159−035, and still further to about 400 s for the coolest pulsators.

Now that we know the photospheric abundances of most PG 1159 stars and have some constraints on their composition profiles, we feel the time is ripe to reexamine the nonadiabatic pulsation properties of "quasi-evolutionary" models of PG 1159 stars. Another motivating factor is the recent availablity of improved radiative (OPAL) opacities for He/C/O/metal mixtures (Iglesias & Rogers 1993). OPAL opacities for H/He/metal mixtures resolved several outstanding discrepancies between observations and theory for Cepheids, RR Lyrae stars, and δ Scuti stars (Andreasen 1988; Simon & Cox 1991; Moskalik, Buchler, & Marom 1992; and Petersen 1992). Given these and other successes we want to see whether inclusion of the OPAL opacities significantly changes the previous driving region constraints based on the Huebner et al. (1977) opacities. We also wish to constrain the composition of the driving region required to produce pulsationally unstable modes out to the longest observed period for models corresponding to several pulsating PG 1159 stars. Further discussions about the expected structure of PG 1159 stars may be found in Wignet et al. (1991), KB, and in articles from recent meetings, such as Vauclair & Sion (1991), Barstow (1993), Koester & Werner (1995).

In the rest of the paper, we describe our models and nonadiabatic pulsation analysis results obtained from them. First, in § 2 we discuss our quasi-evolutionary and static PG 1159 star models and describe the numerical methods we use. In § 3 we present the results of our parametric survey of nonadiabatic pulsation properties of our PG 1159 models and compare them to previous results and current observational constraints in § 4. Finally, in § 5 we present our summary and conclusions.

2. EQUILIBRIUM MODELS

We use both the evolutionary models described by KB and additional static envelope models to fully explore the structural possibilities of models appropriate to the PG 1159 type stars. By using two independent sets of models and pulsation analysis programs, we are better able to assess the model dependence of our conclusions. While our static envelope models are not completely consistent with full stellar evolution models, they allow us to easily explore changes in stellar radius at a given effective temperature. Most of the inconsistencies lie with the structure of the deep interior, which has little effect on the pulsation properties of the high-overtone modes we examine.

2.1. *Evolutionary Models*

We derive our evolutionary models from a 0.6 $M_\odot$ hydrogen-deficient post–AGB model described by KB. We refer the reader to that paper for further details concerning starter models and our version of the white dwarf evolution code (WDEC). Here we will only cover the changes to the input physics made for this work.

Our models include accurate treatments of the equation of state, neutrino losses, opacities, and the effects of chemical pulsation transition zones on the Brunt-Väisälä frequency, as described by KB. Since KB, we added the recent neutrino loss rates of Itoh et al. (1989) and Kohyama et al. (1993). The new neutrino rates are about 5%–10% lower; this does not appreciably affect the evolutionary properties of our models. In addition to the equation of state (EOS) tables used by KB, we also use some new EOS tables for pure C, pure O, and several He/C/O mixtures, kindly made available to us by F. Swenson (Swenson et al. 1996). As expected, the EOS properties of mixtures are different in the partial ionization zone when compared with results from the use of the additive volume method on pure element tables (Fontaine, Graboske, & Van Horn 1977) and Swenson's explicit EOS table for the same mixture. Thus, our results for models using the additive volume EOS must be regarded as preliminary, pending a full set of EOS tables for He/C/O mixtures. Because partial ionization is at least partly responsible for driving the observed pulsations, we require accurate opacities and their derivatives. We use the He/C/O opacity tables of Iglesias, Rogers, & Wilson (1992)

and Iglesias & Rogers (1993) with $Z = 0.001$ for our radiative opacity values, and the conductive opacities of Itoh et al. (1983) in our models. We started out deriving opacities for mixtures by averaging the opacities from the pure element tables, but found that they deviate unacceptably from the opacity values of the explicit table for that mixture or interpolation between several tables. Our numerical experiments show that a two-dimensional cubic spline interpolation routine (kindly supplied by P. Moskalik) provides the smoothest derivatives. For most of our work we use the OPAL opacity tables with $Z = 10^{-3}$; we cover the effects of metallicity on pulsation driving in the next section.

2.2. *Static Models*

We also construct a series of unfitted envelope models (Dziembowski 1977; Moskalik & Dziembowski 1992) utilizing the Fontaine et al. (1977) EOS, along with the oxygen EOS of Kawaler (1993). We use the same OPAL opacity tables used in WDEC, but do not include conductive opacities, which are negligible in the envelope. These models give us the ability to examine the effects of varying the stellar radius on the pulsation properties for a given mass and effective temperature. The growth rates of these models are similar to those of our evolutionary models that have similar effective temperatures and radii, because the contributions to driving and damping occur in the outer layers for the high-overtone g-modes we consider.

2.3. *Pulsation Analysis Programs*

We use three independent nonadiabatic nonradial oscillation (NANRO) analysis codes to determine the pulsation properties of our PG 1159 models. All three codes solve the pulsation equations in a mixed Eulerian-Lagrangian formulation (see Dziembowski 1977; Saio & Cox 1980; Lee & Bradley 1993). All three codes use equivalent independent variables, solve essentially the same pulsation equations, and ignore convective flux perturbations (the frozen-in approximation). Above 120,000 K, the convection zone of our models carries no more than 10% of the flux in the driving region. Below this, convection carries more and more of the flux (up to 75%), so these maximum pulsation periods must be regarded as estimates.

Our pulsation analysis codes use the Saio & Cox (1980) or Dziembowski (1977) formulation of the NANRO equations and employ a second-order Newton-Raphson relaxation technique. One code (GNR1) solves the fully nonadiabatic pulsation equations throughout the model and runs into convergence problems below $\sim$120,000 K due to numerical instabilities of the thermal eigenfunction in the core. The other two nonadiabatic programs (Dziembowski 1977; Lee & Bradley 1993) solve the nonadiabatic pulsation equations in the quasi-adiabatic approximation in the core, and switch to the fully nonadiabatic solution in the outer layers. Neither program has convergence problems in cooler models; the GNR1 and Lee & Bradley code growth rates agree to within a few percent for modes from the same models. We also compared the eigenvalue periods and growth rates to those computed from the eigenfunctions using a variational principle. The periods agree to within about 1%, while the growth rates agree to within a factor of 2; this is comparable to the agreement of these codes when we analyze DB and DA models.

3. NONADIABATIC RESULTS

Here we discuss the nonadiabatic properties of our PG 1159 models and their underlying physical trends. We are concerned with the location of the theoretical instability strip and also the period spectrum of unstable modes. We examine models with different surface compositions, metallicity, stellar radius, and stellar mass. We emphasize models with effective temperatures between 160,000 and 70,000 K, covering the observed temperature range of the GW Vir stars. Almost all of the model sequences we examine have pulsationally unstable modes below 150 s, considerably shorter than any observed in a pulsating PG 1159 star to date. These modes are excited by neutrino losses; we do not consider their growth rates to be reliable because we neglect any nuclear burning shell sources that might be present. If modes with such short periods are found in pulsating PG 1159 stars (but see Hine & Nather 1987), they will offer us a unique opportunity to study regions where plasmon neutrino emissions take place. Until we observationally detect such modes, we do not consider them in our determinations of the theoretical instability strip boundaries. In addition, we compare the maximum unstable period to observations to determine the composition of the driving region required to best match the observed maximum unstable period of about 1000 s.

3.1. *General Properties of Pulsation Driving*

Before discussing results for specific models, we review some general pulsation properties common to all of our models. These include thermal properties of the driving region and the behavior of the eigenfunctions as the models evolve to cooler temperatures. For efficient pulsation driving, the local thermal timescale at the base of the driving region ($\tau_{\rm th}$; see Cox 1980 or Unno et al. 1989) must be similar to the pulsation period (P). In our models, the driving region is located between 4×10^{-8} and $10^{-9}\ M_*$; where the thermal timescale is between 200 and 2000 s (see Table 1). The pulsations are driven primarily by the κ, γ mechanism in our hotter models, so maximum driving occurs near the rapid rise in the temperature derivative of the opacity (κ_T) from its minimum value, located near $10^{-8}\ M_*$. Pulsation driving is more efficient as the slope of the rise in κ_T *and* the depth of its minimum increases. Our hotter models have a second, smaller minimum in κ_T between 10^{-9} and $10^{-10}\ M_*$ which drives short-period ($P < 200$ s) modes. These two driving regions merge in our cooler models, creating a continuous range of unstable modes from low overtones up to the overtone corresponding to $P_{\rm max}$. Below 100,000 K, convection can carry the majority of the flux in the driving region (see Fig. 1), and perturbations to the convective flux (which we do not include) become increasingly important for accurately determining the growth rates.

3.2. *Surface Composition Effects on Pulsation Driving*

In our study, we consider two types of composition profiles. The first set of models has homogeneous profiles extending from the surface to well below the driving region. We do not intend these models to duplicate observed spectra, but they provide the simplest way to explore the effect of chemical composition on pulsation driving. Our other class of models has composition gradients located at various points near the driving region. This includes models with the composition profiles of KB for PG 1159 – 035.

TABLE 1

DRIVING REGION PROPERTIES FOR PURE O ($Z = 0.001$) 0.59 $M_\odot$ MODELS

PARAMETERS	$T_{\rm eff}$ (K)					
	160,300	137,400	119,100	109,400	100,500	75,500
$\log R_*$	9.294	9.214	9.163	9.136	9.112	9.049
$T(\times 10^6$ K)	4.06	3.83	3.80	3.76	3.82	3.84
$P(\times 10^{12}$ dynes)	4.89	5.95	8.47	10.22	13.83	29.31
$-\log(1 - m_r/M_*)$	8.01	8.23	8.28	8.30	8.26	8.19
$(F_{\rm conv}/F_{\rm tot})_{\rm max}$	0.01	0.23	0.61	0.69	0.75	0.66
$\log \tau_{\rm th}$	3.56	3.63	3.85	3.99	4.20	4.84
$\tau_{\rm th}$ at 10^{-9} M_* s	231	518	995	1413	2167	7413
$P_{\rm max}$ (s)	587	640	724	1020	1012	1094

3.2.1. *Homogeneous Composition Models*

We first examine pure C/O models to see what effect changing the C/O mass fraction has on the predicted spectrum of unstable modes (see Table 2). We use explicit EOS tables for each mixture, except for the 10:90 C/O mixture, where we interpolate between the pure O and 50:50 C/O tables. Pure carbon models have only short-period (<150 s) pulsationally unstable modes down to ~70,000 K. Because the unstable modes have periods much shorter than observed, we consider pure carbon models to be pulsationally stable for purposes of this work. When we increase the oxygen mass fraction to 50%, $P_{\rm max}$ starts out at ~150 s in the hottest models, but increases steadily with decreasing effective temperature below 140,000 K. By 10^5 K, $P_{\rm max}$ is over 500 s and reaches a maximum of 700 s in our coolest model at 70,000 K. The 10:90 C/O model has $P_{\rm max}$ values starting at 360 s, increasing to about 1000 s at 90,000 K, where it remains steady to 70,000 K. Our pure oxygen models behave nearly the same as the 10:90 C/O models, except for a larger $P_{\rm max}$ value of ~600 s in our hotter models. Again, the longest $P_{\rm max}$ we obtain is around 1000 s.

We also examine pure C and O models of differing metallicities ($Z = 0$ and $Z = 0.02$) to ascertain the importance of metals in these models. Our pure carbon models show no difference in the spectrum of unstable modes, no matter which metallicity we use. For oxygen, our $Z = 0$ and $Z = 0.001$ results are almost identical, but the longest $P_{\rm max}$ value for our $Z = 0$ models is about 900 s. When $Z = 0.002$, $P_{\rm max}$ lengthens by 20–50 s, meaning that one or two extra overtones are unstable at any given temperature.

TABLE 2

$P_{\rm max}$ FOR DIFFERENT COMPOSITION ($Z = 0.001$) 0.59 $M_\odot$ MODELS

100:000 C/O		50:50 C/O		10:90 C/O		000:100 C/O	
$T_{\rm eff}$ (10^3 K)	$P_{\rm max}$ (s)	$T_{\rm eff}$ (10^3 K)	$P_{\rm max}$ (s)	$T_{\rm eff}$ (10^3 K)	$P_{\rm max}$ (s)	$T_{\rm eff}$ (10^3 K)	$P_{\rm max}$ (s)
156.7	125	157.8	170	160.0	366	160.3	587
151.4	126	151.7	148	151.0	432	151.0	590
138.9	129	137.7	218	140.3	501	137.4	640
129.1	131	128.5	352	129.1	573	129.1	668
121.0	133	120.5	421	120.2	601	119.1	724
109.4	136	111.5	469	110.4	681	109.4	1020
98.9	140	99.8	523	100.0	897	100.5	1012
90.8	144	89.7	581	90.4	1000	89.3	1098
80.2	149	80.5	647	80.4	950	80.0	1104
70.0	157	71.0	698	70.0	994	70.6	1030

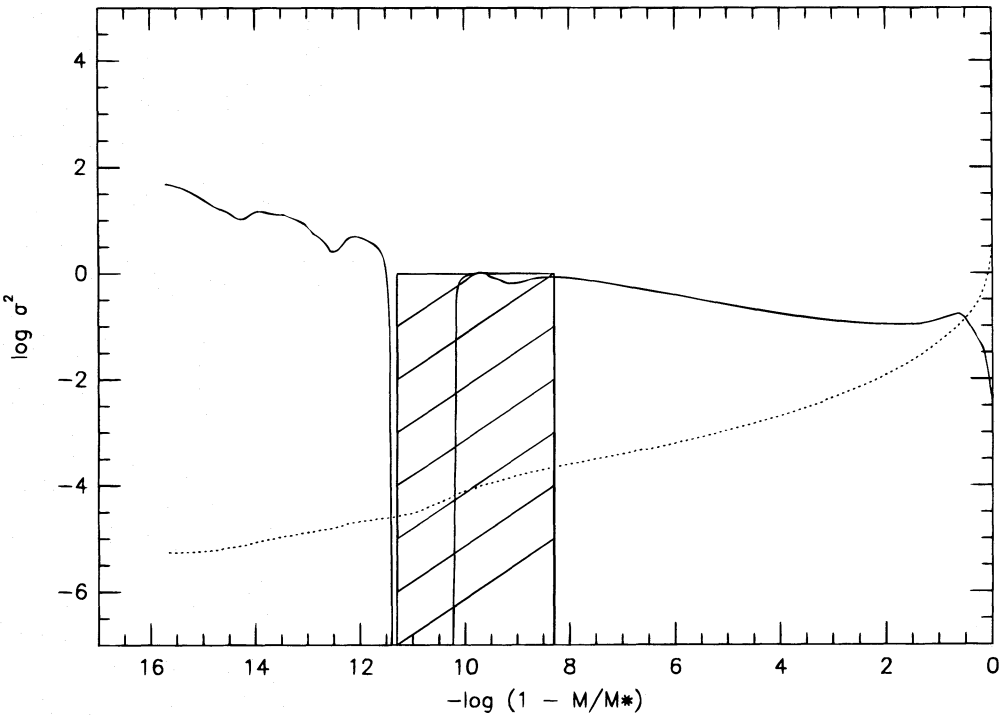

FIG. 1.—Propagation diagram for a typical pre–white dwarf model. The driving region (*hatched area*) includes the convection zone, where the square of the Brunt-Väisälä frequency become negative (between 10^{-10} and 10^{-12} M_*).

In addition, we examined some pure oxygen models with both the old Huebner et al. (1977) opacities and compare them to the OPAL opacity results. The Huebner et al. opacity models have ragged opacity derivatives due to the table edge effects, which affect the depth of the κ_T minimum and the amount of pulsation driving. As a result, the P_{max} values for our Huebner opacity models are about 40–80 s shorter than for an OPAL opacity model at the same effective temperature. The OPAL opacities are greater, especially in the outermost layers above $10^{-10}\ M_*$, and this makes the OPAL models about 10^4 yr older (for pure oxygen) at a given effective temperature. The slower cooling rate of the OPAL opacity models makes their periods about 1% shorter at temperatures near 10^5 K, but this has little effect on the period spacings. This implies that the effective temperature of the best-fitting model derived by KB using models with the Huebner et al. opacities may be slightly off, but the derived mass is secure.

Even with the OPAL opacities and equation of state, we need EOS and opacity tables closely spaced in composition for accurate interpolation of quantities for mixtures. When we use the additive volume technique (Fontaine et al. 1997) for the EOS, and average the pure C and pure O opacities for a 50:50 C/O mixture, we obtain P_{max} values near 150 s at all temperatures. A look at the temperature derivative of the opacity (κ_T) profile (see Fig. 2, top panel) shows the κ_T minimum is deeper when we use the correct EOS and opacity tables, especially below 140,000 K. This leads to greater amounts of driving for a given mode (see Fig. 2, *bottom panel*), and longer period unstable modes.

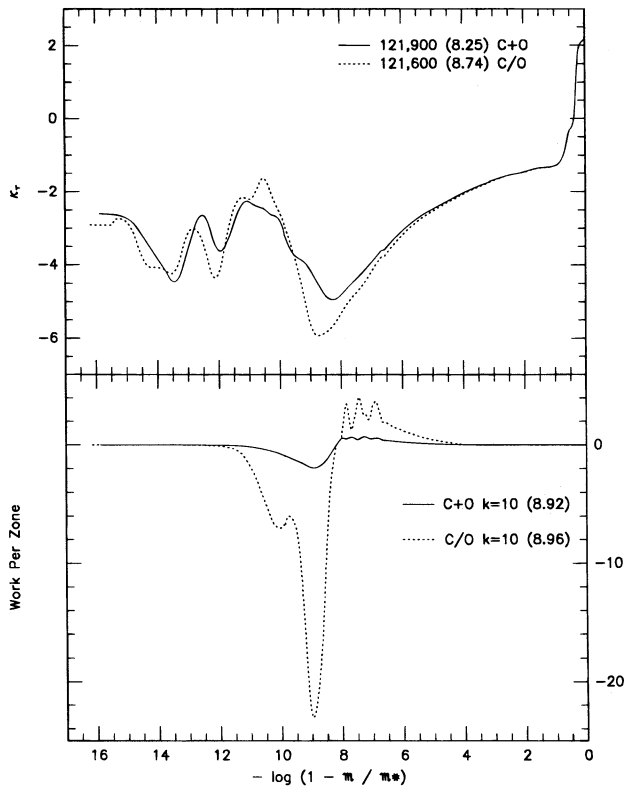

FIG. 2.—Opacity-temperature derivative (κ_T; *upper panel*) and work per zone (*lower panel*) plots for 0.59 $M_\odot$ models composed of 50:50 C/O at ~120,000 K. Models computed with opacities for a 50:50 C/O mixture (*dashed line*) have a deeper κ_T minimum than models with opacities computed from pure C and pure O tables. Numbers in parentheses indicate the location of the κ_T minimum and point of maximum driving in units of $-\log(1 - m_r/M_*)$.

3.2.2. *Composition Gradient Models*

Now we look at models that have composition gradients at or near the driving region to see what effect composition gradients have on pulsation driving. Due to our lack of EOS tables for all of the mixtures of interest, we use the additive volume technique for the EOS variables and average the opacity values from the pure element tables. We therefore consider these results to be tentative. Still, they show trends that are worth following up in future work.

We start with several 0.59 $M_\odot$ models near 140,000 K having a 30:00:70 He/C/O surface that changes to a 10:90 C/O core at varying transition points (see Fig. 3). When the transition point lies between 5×10^{-8} and $10^{-6}\ M_*$, P_{max} is between 500 and 600 s. We also obtain a P_{max} of about 500 s when we replace the He/O surface layer with a 30:60:10 He/C/O surface layer with a transition point at $5 \times 10^{-7}\ M_*$. However, when we move the transition point for the 30:60:10 He/C/O surface layer around, we find little pulsation driving, and P_{max} values closer to 150 s. In both cases, the changing composition of the transition region acts to deepen the minimum in κ_T that we normally see from partial ionization, increasing P_{max}. If we misplace the transition region so the minimum caused by the composition change does not coincide with the κ_T minimum due to partial ionization, the driving enhancement does not occur, and we typically see P_{max} values of about 150 s.

As a final test, we put a PG 1159 spectral type surface layer (27:58:15 He/C/O) on a model with a pure oxygen driving region. We compare these models to similar pure oxygen models and find P_{max} values that are similar, at about 640 s for models near 140,000 K. This confirms that the photospheric composition is not important for determining the driving properties of our models, and that we can have a carbon-rich surface composition overlying an oxygen-rich driving region, so long as we have a physically plausible mechanism for maintaining the chemical composition profile. The real challenge is our need for an oxygen-rich driving region overlying the seismologically determined composition transition zone at $\sim 4 \times 10^{-3}\ M_*$ within the star; this goes against physical intuition. We emphasize that our driving region transition zones have nothing to do with the seismologically detected transition zones of KB and Kawaler et al. (1995). Indeed, the driving region transition zones have an insignificant effect on the predicted pulsation periods, making it entirely possible that there is an He/C/O transition zone just below the driving region that is seismically undetectable.

3.3. *Effect of Stellar Radius on Pulsation Driving*

We use static envelope models to investigate the effect changing the stellar radius of a model has on P_{max}. The P_{max} values for our static models agree with evolutionary model values with the same radii to within 70 s. We find a large increase in P_{max} when we increase the radius of our static envelopes. At 120,000 and 132,000 K, P_{max} doubles when we increase the radius by 50%. At 144,000 K, P_{max} increases by a factor of 2.5 for a 70% radius increase (see Table 3 and Fig. 4). Physically, the increase in P_{max} with increasing radius is due to the decreased degeneracy in the outer layers of the larger models. The core conditions are unchanged, so these models are more centrally condensed, and a given

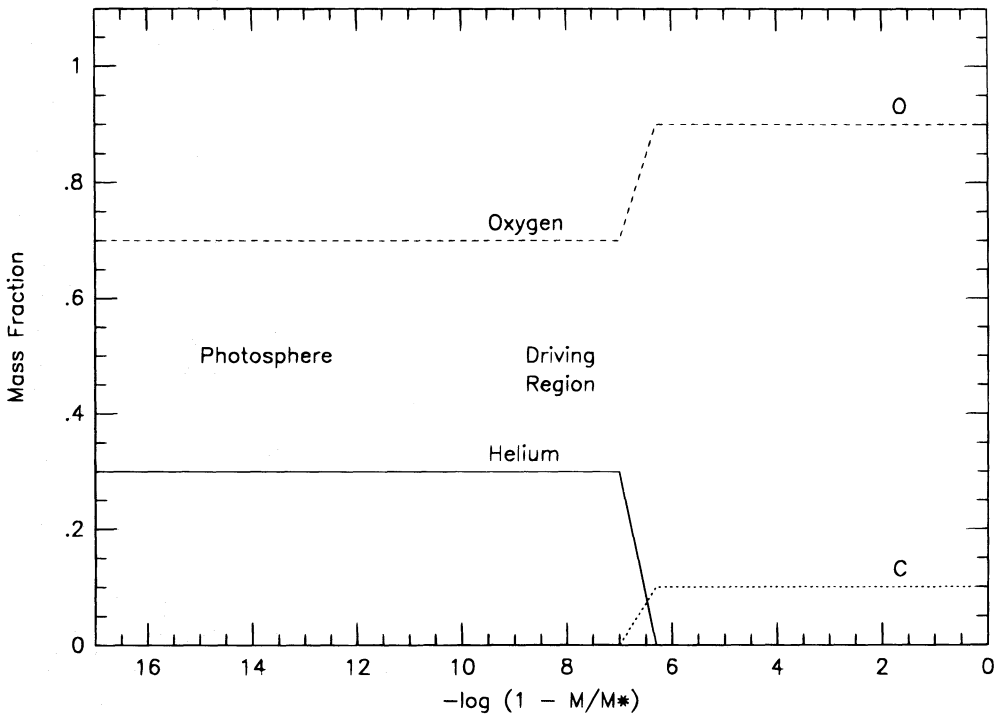

FIG. 3.—Composition profile for a typical model with a 30:00:70 He/C/O surface composition and a 10:90 C/O core

overtone mode will have its energy concentrated closer to the core, mimicking the pulsation properties of a lower overtone mode in a model that has a smaller radius.

3.4. *Effect of Stellar Mass on Pulsation Driving*

Finally, we examine evolutionary models with stellar masses ranging from 0.50 to 0.65 $M_\odot$ for a 50:50 C/O composition to determine the effect of stellar mass on the theroetical P_{max} values. As the stellar mass decreases there is an increase in P_{max} due to the decreased degeneracy (and increased radius) of the lower mass models. This effect is greater in hotter models, where the radius and degeneracy differences are the greatest. Above 140,000 K, the 0.59 and 0.65 $M_\odot$ models only have short-period modes excited; below this, P_{max} rapidly increases until about 100,000 K (see Table 4 and Fig. 5). The dramatic increase in P_{max} in the more massive models is due to the disappearance of a local maximum in κ_T near 3×10^{-10} M_*. The maximum flattens out and goes away by about 140,000 K in 0.59 $M_\odot$ models, greatly expanding the depth and span of the κ_T minimum, allowing many more modes to be unstable. This accounts for the dramatic change in P_{max} with stellar mass at about 140,000 K. At $\sim 10^5$ K, there is about a 100 s decrease in P_{max} for every 0.05 $M_\odot$ increase in stellar mass.

All except our 0.50 $M_\odot$ models have increasing P_{max} with decreasing T_{eff}, whereas our 0.50 $M_\odot$ models have a nearly constant P_{max} of ~ 800 s between 145,000 and 70,000 K. The

TABLE 4

P_{max} FOR 50:50 C/O ($Z = 0.001$), DIFFERENT STELLAR MASS MODELS

0.50 $M_\odot$		0.55 $M_\odot$		0.59 $M_\odot$		0.65 $M_\odot$	
T_{eff} (10^3 K)	P_{max} (s)	T_{eff} (10^3 K)	P_{max} (s)	T_{eff} (10^3 K)	P_{max} (s)	T_{eff} (10^3 K)	P_{max} (s)
...	...	161.4	81	157.8	170	159.2	152
144.2	831	151.7	82	151.7	148	150.0	154
139.3	803	138.4	421	138.7	218	139.0	156
128.5	777	128.8	494	128.5	352	130.0	179
120.5	778	120.5	544	120.5	421	118.6	281
108.6	810	109.6	597	111.2	469	110.4	345
100.0	817	100.9	630	99.8	523	100.7	412
91.0	825	90.4	668	89.7	581	90.4	490
80.9	869	80.2	736	80.5	647	80.7	554
70.1	890	70.1	786	71.0	698	70.5	631

TABLE 3

P_{max} FOR 10:90 C/O ($Z = 0.001$) 0.59 $M_\odot$ STATIC ENVELOPE MODELS

T_{eff} = 120,300 K			T_{eff} = 131,800 K			T_{eff} = 144,500 K		
log R_* (cm)	log ($L/L_\odot$)	P_{max} (s)	log R_* (cm)	($L/L_\odot$)	P_{max} (s)	log R_* (cm)	log ($L/L_\odot$)	P_{max} (s)
...	...	...	...	...	...	9.407	2.72	1020
9.367	2.32	1117	9.367	2.48	1005	9.367	2.64	868
9.326	2.24	980	9.327	2.40	875	9.327	2.56	739
...	...	...	9.317	2.38	845	...	...	...
...	...	...	9.287	2.32	759	9.287	2.48	624
9.246	2.08	756	9.246	2.24	656	9.247	2.40	523
9.207	2.00	664	...	...	...	9.207	2.32	434
9.167	1.86	583	9.167	2.08	491	9.167	2.24	350

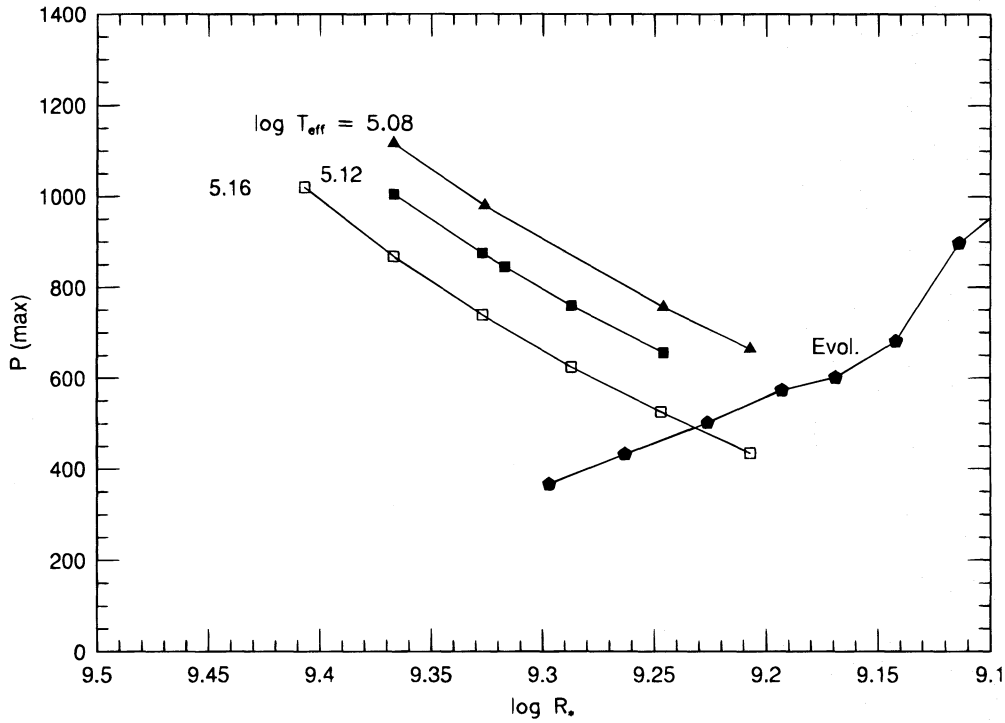

FIG. 4.—P_{max} as a function of stellar radius and effective temperature for 10:90 C/O 0.59 $M_\odot$ static and evolutionary models. Models with larger radii are less degenerate, allowing longer period modes to be pulsationally unstable (log T_{eff} values are indicated next to each static model sequence).

near-constant P_{max} is due to the counterbalancing effects of gravitational contraction pushing higher overtone eigenfunctions out of the region of maximum driving and the lengthening of the thermal timescale within the driving region.

4. COMPARISON TO PREVIOUS RESULTS AND OBSERVATIONS

There are few other calculations of nonadiabatic pulsation properties of models appropriate to GW Vir stars, and

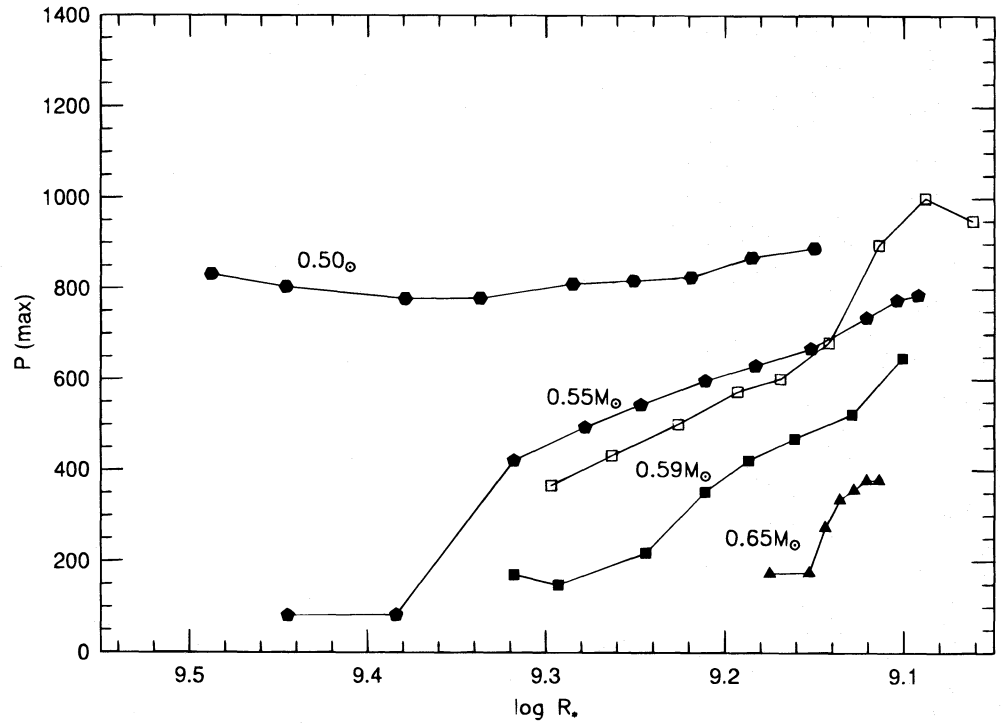

FIG. 5.—P_{max} as a function of stellar radius for different mass 50:50 C/O models. P_{max} is nearly constant at all effective temperatures in our 0.50 $M_\odot$ mass models, while higher mass models show a rapidly increasing P_{max} as the driving region becomes deeper. 0.59 $M_\odot$ with 10:90 C/O composition (*open squares*) have P_{max} values at least 100 s longer than 50:50 C/O 0.59 $M_\odot$ models with the same radii (*filled squares*).

most of these are by Starrfield, Cox, and their collaborators. Starrfield et al. (1983, 1984) and Stanghellini et al. (1991) examine 0.6 $M_\odot$ structure models with differing C/O compositions and obtain results in general agreement with ours, especially in their later papers. Our evolutionary models tend to have shorter P_{max} values, which we expect because the radii of our models are a good bit smaller than theirs, especially for the hotter models. When we match the radii and effective temperatures of our 10:90 C/O envelope models with theirs, our models have longer P_{max} values by virtue of their more oxygen-rich driving regions. Thus, while we cannot compare models in detail, our trends and theirs are consistent.

Our second goal is to compare our theoretical instability strips and P_{max} values to observational limits to see what constraints they offer on the likely composition of the driving region. We have Whole Earth Telescope (WET) data for PG 1159−035 (Winget et al. 1991) and PG 2131+066 (Kawaler et al. 1995), which lie on opposite ends of the pulsationally unstable region. We also have good single-site data for PG 1707+427 (Fontaine et al. 1991), which has an intermediate temperature. Winget et al. (1991) and Fontaine et al. (1991) find $l = 1$ modes for PG 1159−035 and PG 1707+427, with periods up to ∼1000 s, while the coolest star (PG 2131+066) has no unstable modes longer than 510 s (Kawaler et al. 1995).

Our evolutionary models have considerably shorter P_{max} values than observed for PG 1159−035 and PG 1707+427. Even our pure oxygen 0.59 $M_\odot$ evolutionary models at 140,000 K have P_{max} values of only ∼600 s. If we look at our largest static models at ∼140,000 K, they have P_{max} values near 1000 s, but this requires a 10:90 C/O composition. Put together, this suggests that PG 1159−035's progenitor had an evolutionary history that gives it a larger radius than the quasi-evolutionary models of KB and/or that the contraction rate of the envelope is greater than predicted by KB. This sounds improbable, but our pure oxygen models do not have composition interpolation uncertainties and we are using OPAL data for both the EOS and opacities, so it is unlikely that we are facing serious input physics problems. We also feel it quite likely that the driving region is dominated by oxygen or that a strong composition gradient lies within the driving region, because even our largest 10:90 C/O static envelope has P_{max} right at 1000 s. The only way we see to reduce the oxygen mass fraction of the driving region is to further increase the radius of our models; however, at some point, the radius increase will not work because the excellent match between the observed and theoretical periods will deteriorate.

In addition to removing the discrepancy between the observed and theoretical P_{max}, a larger radius model for PG 1159−035 would also be better able to match the observed rate of period change ($-2.49 \pm 0.06 \times 10^{-11}$ s s^{-1}) for the 516 s mode of PG 1159−035. Experiments with evolutionary models having artificially increased radii bear out our expectations: P_{max} increases, the magnitude of the best-fitting dP/dt value of Kawaler & Bradley (1994) increases by a factor of 3, and the pulsation periods are essentially unchanged from those of the smaller radius model. While suggestive, this experiment says nothing about how one makes a model evolve from the AGB to the PG 1159 phase with a P_{max} and dP/dt value that matches the observations. To see what effect a modified model would have on the seismological determination, we assume we can vary the effective temperature slightly to retain the period match of Kawaler & Bradley. We find that a 0.59 $M_\odot$ model at about 140,000 K with a 30% larger radius will have a radius of 0.033 $R_\odot$, a luminosity of $\log (L/L_\odot) = 2.65$, the distance would increase to 660 pc, and $\log g$ would drop to 7.16. These values are still well within the spectroscopic error bars. A word of warning: we are *not* saying the values of Kawaler & Bradley are wrong; we merely suggest it will be worthwhile to examine models for PG 1159−035 with radii larger than predicted by the models we present here.

PG 1707+427 has an intermediate temperature of about 100,000 K, with a mass somewhere between 0.6 and 0.7 $M_\odot$. Only oxygen-rich ($\gtrsim$90%) quasi-evolutionary 0.59 $M_\odot$ models at 100,000 K have P_{max} values near 1000 s. Our static model results suggest we can reduce the oxygen content of the driving region in exchange for an appropriate increase in the radius of our models. The allowable range of radii and oxygen mass fractions will be strongly dependent on the exact stellar mass. If it is near 0.7 $M_\odot$, we will probably need a nearly pure oxygen driving region and an increased radius to obtain a P_{max} near 1000 s. An accurate seismological mass for PG 1707+427 should be available soon from the WET data set; this will go a long way toward constraining the combination of oxygen enhancement and radius increase required of our models to match observations.

By contrast, we do not require a radius increase for PG 2131+066, which is a 0.61 $M_\odot$ star with a much cooler T_{eff} of 80,000 K and a 50:30:20 He/C/O photosphere. At 80,000 K, our 50:50 C/O driving region 0.6 $M_\odot$ models have longer P_{max} values than observed; we can also match the observed P_{max} with several of our composition gradient models. However, the 150 s P_{max} of our 30:60:10 models suggest we need a slight oxygen enhancement (relative to the photosphere) in the driving region. This conclusion is probably true for PG 0122+200 as well; the single-site data of Hill, Winget, & Nather (1987) has the longest period at about 610 s, and Dreizler, Werner, & Heber (1995) give $T_{eff} = 75{,}000$ K. We emphasize that we are not forced to invoke an increased stellar radius to boost our theoretical P_{max} values for PG 2131+066 or PG 0122+200. Most likely, this is because the longer cooling time for these stars gives gravitational contraction enough time to bring the actual stellar radii close to what we predict with our evolutionary models.

In closing, a comparison of our results to observations leads to several provocative suggestions. A comparison of our results to the data for PG 1159−035 shows our evolutionary model P_{max} values are about 400 s shorter than the observed value, which we believe can be removed by assuming the evolutionary models have a radius about 30% larger than that predicted by the seismological results of KB. Some increase in the radius of our models for PG 1707+427 is probably required, but we must await an accurate seismological mass to determine the extent. We require less drastic revisions to our models to duplicate the observed P_{max} values of PG 0122+200 and PG 2131+066. The greater cooling ages of these stars imply that any radius increase needed to reduce the oxygen content of the driving region is probably small. Also, our results clearly indicate that the observed surface abundances are *not* present in the driving region; the lack of oxygen at the photosphere would strangle pulsations in the driving region.

5. SUMMARY AND CONCLUSIONS

In spite of what we know about the surface composition and internal structure of the PG 1159 stars, they remain an enigma, because several poorly understood processes play important roles in determining the structure of their outer layers. These include convection, mass loss, selective radiative levitation, and diffusion. If we can determine the chemical composition of the driving region in the pulsating PG 1159 stars, we can provide important composition constraints between the photosphere and the interior. A better knowledge of the chemical composition profile with depth will help us assess the relative importance of the aforementioned physical processes affecting the abundances. We examine the pulsation spectrum of linearly unstable modes because the alternative explanation of excitation via parametric resonances (Dziembowski 1982) requires that frequencies satisfy the condition $\nu' \approx 2\nu_0$, which we do not observe. Here we examine the changes to the spectrum of theoretically unstable modes as a function of chemical composition and stellar structure using the new OPAL opacities (Iglesias & Rogers 1993). The switch to OPAL opacities from the Huebner et al. opacities removes some interpolation problems in the derivatives and produces $P_{\max}$ values that are longer by 40–80 s.

Our quasi-evolutionary C/O models require at least a 50% oxygen composition in the driving region to have pulsationally unstable modes longer than 200 s. Pure oxygen models have $P_{\max}$ values up to 1000 s, but only when $T_{\rm eff} \lesssim$ 110,000 K. Under favorable circumstances, models with a composition gradient in or near the driving region (at $\sim 10^{-8}\ M_*$) can drive modes with periods over 500 s. We must confirm this result with both EOS data and opacities that are valid for the changing compositions, because the additive volume method we use for most of our EOS values is inadequate for partially ionized mixtures. We find a dramatic increase in $P_{\max}$ with increasing stellar radius, whether we increase the radius of our static models at constant mass or decrease the mass of our evolutionary models, because the driving region becomes less compact. For example, a 50% increase in the stellar radius of our static models doubles the theoretical $P_{\max}$ value. Our hottest evolutionary models show dramatic differences in $P_{\max}$, because higher mass hot models have too small a κ_T minimum for κ-effect driving to be strong enough to drive long-period modes. Our cooler models have sufficient pulsation driving at all masses, and we find approximately a 100 s increase in $P_{\max}$ with every 0.05 $M_\odot$ decrease in stellar mass.

Our evolutionary models tend to predict $P_{\max}$ values shorter than observed. To match the longest period unstable mode ($\sim$1000 s) seen in PG 1159−035, our results imply that we need a combination of an oxygen-rich driving region and an increased stellar radius in our models, possibly up to 30% larger. PG 1707+427 also requires a combination of an oxygen-rich driving region and an increased stellar radius, but uncertainties in the stellar mass prevent us from determining whether the mismatch is as severe as for PG 1159−035. We can match the longest period ($\sim$510 s) mode seen in PG 2131+066 using 50:50 C/O models, although we cannot rule out the presence of small amounts of helium in the driving region. However, we can rule out helium- and carbon-rich driving regions for the pulsating PG 1159 stars, as these models have $P_{\max}$ values of 200 s or less, far shorter than observed. Further work with larger radius evolutionary models and accurate EOS tables for He/C/O mixtures will help us further constrain the possible compositions of the driving regions.

Based on a comparison of our results to observations and other theoretical studies, we suggest the following picture to explain the observed trend of pulsation driving in the GW Vir stars. The observed trend of decreasing periods for the largest amplitude modes with decreasing $T_{\rm eff}$ is opposite to our trend of $P_{\max}$ with $T_{\rm eff}$. As a result, we believe that either the composition of the driving region changes as these stars cool, or the star is contracting from larger than predicted radii more rapidly than our current models suggest, or both. Theoretical studies of diffusion in pre–white dwarf envelope models (Vauclair 1989; Unglaub & Bues 1995) show complex variations in CNO abundances with depth and changes in the CNO profiles as the models cool. Current models that include mass loss, diffusion, and radiative levitation do not predict the correct abundances of He, C, N, and O, however. Much theoretical work—especially with mass loss—must still be done here. Observations (Leuenhagen 1995) show the mass-loss rates are small; for RXJ 2117+3412 and PG 1159−035, they are less than $10^{-9}\ M_*\ {\rm yr}^{-1}$. Our *speculation* is that the hottest pulsators (RXJ 2117+3412 and PG 1159+035) probably are considerably larger than our quasi-evolutionary models predict and they have the most oxygen-enriched driving regions. As we move to cooler GW Vir stars, oxygen is depleted from the driving region just fast enough to maintain $P_{\max}$ at $\sim$1000 s (as we see for PG 1707+427) while the increasing degeneracy and mode trapping of the star push the eigenfunctions outward, so that the largest amplitude unstable mode is at 450 s for PG 1707+427 rather than the longer 517 s for PG 1159−035. Some combination of surface convection, mass loss, radiative levitation, and diffusion must be keeping the surface abundances virtually identical between 140,000 and 100,000 K, as we see in the spectroscopic abundances derived for PG 1159−035 and PG 1707+427. Diffusion continues to change the driving region composition until helium and carbon are enriched enough to shut off pulsation driving by about 70,000 K. By this point, mass loss should be negligible, and diffusion should be making the surface more and more helium-enriched, as recent observed abundance analyses suggest (Dreizler et al. 1995).

Clearly, the nonpulsating PG 1159 stars have different driving region compositions than the pulsators, despite our seeing spectroscopic "twins," such as PG 1159−035 and PG 1520+525 at 140,000–150,000 K along with PG 1707+427 and PG 1424+535 near 100,000 K. Two observational tests may clarify the driving region composition mystery somewhat. First, a comparison of the chemical abundances in the inner portions of the nebulae around RXJ 2117+3412 (pulsator) and PG 1520+525 (nonpulsator) will tell us about material ejected soon after the final shell flash. A comparison of abundance gradients with the nebula and the current photospheres would also tell us how drastic the chemical composition changes during the final phases of mass loss are. Second, we should compare the abundances of trace elements for PG 1520+525 and PG 1159−035 to see whether we can find any differences in their atmospheric structure that we can use to constrain future evolutionary model envelope calculations. In this vein, we note that Werner & Rauch (1994) did not find neon

in PG 1159−035, consistent with model atmosphere predictions. These tests may help us determine what differences in the final thermal pulse and subsequent mass-loss history are responsible for the presence of pulsators and nonpulsators among the PG 1159 spectroscopic class of stars. We believe these observations will show subtle differences pointing to a less oxygen-rich driving region or the lack of a composition gradient in the driving region that prevents pulsations in PG 1520+525 and PG 1424+535.

We are grateful to J. A. Guzik, S. D. Kawaler, P. A. Moskalik, R. E. Nather, D. E. Winget, K. Werner, and M. A. Wood for their encouragement, discussions, and comments on earlier drafts of this paper. We also thank the referee, K. Werner, for additional comments that improved the presentation of this paper. We also thank F. J. Swenson for computing EOS tables for He/C/O mixtures that greatly aided our work. Part of this work was done when P. A. B. was a visitor at the Copernicus Astronomical Center; he gratefully acknowledges their hospitality and support. P. A. B. also gratefully acknowledges the McDonald Observatory Council for travel funds to Poland. This research was supported by the National Science Foundation under grant 90-14655 through the University of Texas and McDonald Observatory, by a Los Alamos National Laboratory Director's Postdoctoral Fellowship, and by the Polish National Committee for Scientific Research grant 2-1185-91-01.

REFERENCES

Andreasen, G. K. 1988, A&A, 201, 72
Appleton, P. N., Kawaler, S. D., & Eitter, J. J. 1993, AJ, 106, 1973
Barstow, M. A., ed. 1993, in White Dwarfs: Advances in Observations and Theory (Dordrecht: Kluwer)
Cox, A. N. 1986, in Highlights Astron., ed. J.-P. Swings (Dordrecht: Reidel), 229
Cox, J. P. 1980, Theory of Stellar Pulsation (Princeton: Princeton Univ. Press)
Dreizler, S., Werner, K., & Heber, U. 1995, White Dwarfs, ed. D. Koester & K. Werner (Berlin: Springer), 160
Dzeimbowski, W. 1977, Acta Astron., 27, 95
———. 1982, Acta Astron., 32, 147
Fontaine, G., Bergeron, P., Vauclair, G., Brassard, P., Wesemael, F., Kawaler, S. D., Grauer, A. D., & Winget, D. E. 1991, ApJ, 378, L49
Fontaine, G., Graboske, H. C., Jr., & Van Horn, H. M. 1977, ApJS, 35, 293
Hill, J. A., Winget, D. E., & Nather, R. E. 1987, in IAU Colloq. 95, The Second Conference on Faint Blue Stars, ed. A. G. D. Philip, D. S. Hayes, & J. Liebert (Schenectady: Davis), 627
Hine, B. P., & Nather, R. E. 1987, in IAU Colloq. 95, The Second Conference on Faint Blue Stars, ed. A. G. D. Philip, D. S. Hayes, & J. Liebert (Schenectady: Davis), 619
Huebner, W. F., Merts, A. L., Magee, N. H., & Argo, M. F. 1977, Astrophysical Opacity Library, Los Alamos Sci. Lab. Rep., LA-6760-M
Iglesias, C. A., & Rogers, F. J. 1993, ApJ, 412, 752
Iglesias, C. A., Rogers, F. J., Wilson, B. G. 1992, ApJ, 397, 717
Itoh, N., Adachi, T., Nakagawa, M., Kohyama, Y., & Munkata, H. 1989, ApJ, 339, 354; erratum ApJ, 360, 741 (1990)
Itoh, N., Mitake, S., Iyetomi, H., & Ichimaru, S. 1983, ApJ, 273, 774
Jacoby, G. H., & Van De Steene, G. 1995, AJ, 110, 1285
Kawaler, S. D. 1993, ApJ, 404, 294
Kawaler, S. D., & Bradley, P. A. 1994, ApJ, 427, 415 (KB)
Kawaler, S. D., et al. 1995, ApJ, 450, 350
Koester, D., & Werner, K., eds. 1995, White Dwarfs (Berlin: Springer)
Kohyama, Y., Itoh, N., Obama, A., & Mutoh, H. 1993, ApJ, 415, 267
Kwitter, K. B., Massey, P., Congdon, C. W., & Pasachoff, J. M. 1989, AJ, 97, 1423
Lee, U., & Bradley, P. A. 1993, ApJ, 418, 855
Leuenhagen, U. 1995, White Dwarfs, ed. D. Koester & K. Werner (Berlin: Springer), 205
Méndez, R. H., Gathier, R., Simon, K. P., & Kwitter, K. B. 1988, A&A, 198, 287
Moskalik, P., Buchler, J. R., & Marom, A. 1992, ApJ, 385, 685
Moskalik, P., & Dziembowski, W. A. 1992, A&A, 256, L5
Peterson, J. O. 1992, A&A, 265, 555
Reynolds, R. J. 1987, ApJ, 315, 234
Saio, H., & Cox, J. P. 1980, ApJ, 236, 549
Simon, N. R., & Cox, A. N. 1991, ApJ, 376, 717
Stanghellini, L., Cox, A. N., & Starrfield, S. G. 1991, ApJ, 383, 766
Starrfield, S. G., Cox, A. N., Hodson, S. W., & Pesnell, W. D. 1983, ApJ, 268, L27
Starrfield, S. G., Cox, A. N., Kidman, R. B., & Pesnell, W. D. 1984, ApJ, 281, 800
———. 1985, ApJ, 293, L23
Swenson, F. J., VandenBerg, D. A., Alexander, D. R., & Irwin, A. W. 1996, in preparation
Unglaub, K., & Bues, I. 1995, in White Dwarfs, ed. D. Koester & K. Werner (Berlin: Springer), 118
Unno, W., Osaki, Y., Ando, H., Saio, H., & Shibahashi, H. 1989, Nonradial Oscillations of Stars (2d ed.; Tokyo: Univ. Tokyo Press)
Vauclair, G. 1989, in IAU Colloq. 114, White Dwarfs, ed. G. Wegner (Berlin: Springer), 176
———. 1990, in Proc. Oji Int. Seminar, Progress of Seismology of the Sun and Stars, ed. Y. Osaki & H. Shibahashi (Berlin: Springer), 437
Vauclair, G., & Simon, E. M., eds. 1991, Proc. Seventh European Workshop on White Dwarfs (NATO ASI Ser.; Dordrecht: Kluwer)
Werner, K. 1993, in White Dwarfs: Advances in Observations and Theory, ed. M. A. Barstow (Dordrecht: Kluwer), 67
———. 1995, A&A, submitted
Werner, K., & Rauch, T. 1994, A&A, 284, L5
Werner, K., Rauch, T. Dreizler, S., & Heber, U. 1995, in IAU Colloq. 155, Astrophysical Applications of Stellar Pulsation, ed. R. S. Stobie & P. A. Whitelock (ASP Conf. Ser. 83) (Provo: ASP), 96
Winget, D. E., et al. 1991, ApJ, 378, 326